

Multi-Photon Single and Double Ionization of Complex Atoms by Ultrashort Intense Laser Pulses

K. Bartschat, X. Guan, C.J. Noble, B.I. Schneider, and O. Zatsarinny

Abstract We present an *ab initio* and nonperturbative time-dependent approach to describe the response of a general atom to intense few-cycle laser pulses. After using a highly flexible *B*-Spline *R*-matrix method to generate field-free Hamiltonian and electric dipole matrices, the initial state is propagated in time using an efficient Arnoldi–Lanczos scheme. The method is illustrated with results for excitation and single ionization of Ne and Ar, as well as double ionization of He in a two-color pump-probe arrangement.

1 Introduction

As noted in the cover article for a recent special issue of *Journal of Physics B* [1], “we are [currently] witnessing a revolution in photon science, driven by the vision to time-resolve ultra-fast electronic motion in atoms, molecules, and solids. . .” In-

K. Bartschat

Department of Physics and Astronomy, Drake University, Des Moines, IA 50311, USA, e-mail: klaus.bartschat@drake.edu

X. Guan

Department of Physics and Astronomy, Drake University, Des Moines, IA 50311, USA , e-mail: xiaoxu.guan@drake.edu

C.J. Noble

Computational Science & Engineering Dept., Daresbury Laboratory, Warrington WA4 4AD, UK, e-mail: cjn@maxnet.co.nz

B.I. Schneider

Physics Division, National Science Foundation, Arlington, VA 22230, USA, e-mail: bschneid@nsf.gov

O. Zatsarinny

Department of Physics and Astronomy, Drake University, Des Moines, IA 50311, USA, e-mail: oleg.zatsarinny@drake.edu

deed, the ongoing development of ultra-short and ultra-intense light sources based on high-harmonic generation and free-electron lasers is providing new ways to generate optical pulses capable of probing dynamical processes that occur on attosecond time scales. These capabilities promise a revolution in our microscopic knowledge and understanding of matter [2].

Over the past few years, our group has been working on the development of a general *ab initio* theoretical approach to describe short-pulse intense laser interactions with atoms, which is applicable to complex targets beyond (quasi) two-electron systems. In recent papers [3–5], we outlined how field-free Hamiltonian and electric dipole matrices generated with the highly flexible *B*-Spline *R*-matrix (BSR) [6] suite of codes may be combined with an efficient Arnoldi–Lanczos time propagation scheme to calculate multiphoton excitation as well as single and even double ionization, albeit the latter so far has been restricted to the helium target. A computer code is also publicly available [7].

In this contribution, we briefly summarize the computational method and then present a number of examples to demonstrate the feasibility of the approach. In addition to showing results for excitation and single ionization of Ne and Ar atoms by individual laser pulses of variable length, intensity, and central photon energy, we investigate pump-probe processes in He involving two XUV laser pulses whose time delay is varied. This allows us to visualize the competition between direct and sequential double ionization as a function of the time delay.

Unless specified otherwise, atomic units (a.u.) are used in this manuscript.

2 Computational Approach

We start with the time-dependent Schrödinger equation

$$\begin{aligned} i \frac{\partial}{\partial t} \Psi(\mathbf{r}_1, \dots, \mathbf{r}_N; t) \\ = [H_0(\mathbf{r}_1, \dots, \mathbf{r}_N) + V(\mathbf{r}_1, \dots, \mathbf{r}_N; t)] \Psi(\mathbf{r}_1, \dots, \mathbf{r}_N; t) \end{aligned} \quad (1)$$

for the N -electron wavefunction $\Psi(\mathbf{r}_1, \dots, \mathbf{r}_N; t)$, where $H_0(\mathbf{r}_1, \dots, \mathbf{r}_N)$ is the field-free Hamiltonian containing the kinetic energy of the N electrons, their potential energy in the field of the nucleus, and their mutual Coulomb repulsion, while

$$V(\mathbf{r}_1, \dots, \mathbf{r}_N; t) = \sum_{i=1}^N \mathbf{E}(t) \cdot \mathbf{r}_i \quad (2)$$

represents the interaction of the electrons with the laser field $\mathbf{E}(t)$ in the dipole length form. This gauge is generally preferable for complex atoms, for which highly accurate wavefunctions are very difficult to obtain and the region near the nucleus would need to be very well described for the velocity or acceleration gauges to be applicable. For an extended discussion of using different gauges for the helium

target, we refer to the recent paper by Hutchinson et al. [8], as well as the references therein.

The tasks to be carried out in order to computationally solve this equation and to extract the physical information of interest are:

1. Generate a representation of the field-free Hamiltonian and its eigenstates; these include the initial bound state, other bound states, autoionizing states, as well as single-continuum and double-continuum states to represent electron scattering from the residual ion.
2. Generate the electric dipole matrices to represent the coupling to the laser field.
3. Propagate the initial bound state until some time after the laser field is turned off.
4. Extract the physically relevant information from the final state.

The solution of the TDSE requires an accurate and efficient generation of the Hamiltonian and electron–field interaction matrix elements. In order to achieve this goal, we approximate the time-dependent wavefunction as

$$\Psi(\mathbf{r}_1, \dots, \mathbf{r}_N; t) \approx \sum_q C_q(t) \Phi_q(\mathbf{r}_1, \dots, \mathbf{r}_N). \quad (3)$$

The $\Phi_q(\mathbf{r}_1, \dots, \mathbf{r}_N)$ are a set of time-independent N -electron states formed from appropriately symmetrized products of atomic orbitals. They are expanded as

$$\begin{aligned} & \Phi_q(\mathbf{r}_1, \dots, \mathbf{r}_N) \\ &= \mathcal{A} \sum_{c,i,j} a_{ijcq} \Theta_c(x_1, \dots, x_{N-2}; \hat{\mathbf{r}}_{N-1} \sigma_{N-1}; \hat{\mathbf{r}}_N \sigma_N) R_i(r_{N-1}) R_j(r_N). \end{aligned} \quad (4)$$

Here \mathcal{A} is the antisymmetrization operator, $\Theta_c(x_1, \dots, x_{N-2}; \hat{\mathbf{r}}_{N-1} \sigma_{N-1}; \hat{\mathbf{r}}_N \sigma_N)$ are channel functions involving the space and spin coordinates (x_i) of $N - 2$ core electrons coupled to the angular ($\hat{\mathbf{r}}$) and spin (σ) coordinates of the two outer electrons, $R_i(r)$ is a radial basis function, and the a_{ijcq} are expansion coefficients. Although resembling a close-coupling ansatz with two continuum electrons, the expansion (4) contains bound states and singly ionized states as well. In general, the atomic orbitals, $R_i(r)$, are not orthogonal to one another or to the orbitals used to describe the atomic core. If orthogonality constraints are imposed on these functions, additional terms would need to be added to the expansion to relax the constraints. This possibility still exists as an option in our computer code.

When the expansion (3) is inserted into the Schrödinger equation, we obtain

$$iS \frac{\partial}{\partial t} \mathbf{C}(t) = [\mathbf{H}_0 + E(t)\mathbf{D}] \mathbf{C}(t), \quad (5)$$

where S is the overlap matrix of the basis functions, \mathbf{H}_0 and \mathbf{D} are representations of the field-free Hamiltonian and the dipole coupling matrices, and $\mathbf{C}(t)$ is the time-dependent coefficient vector in (3).

The price to pay for the flexibility in the BSR approach, at least initially, is the representation of the field-free Hamiltonian and the dipole matrices in a nonorthog-

onal basis. To solve this problem, we use a transformation into the eigenbasis by solving the field-free generalized eigenvalue problem first. Details can be found in [4]. In addition to simplifying the definition of the initial state and the extraction of the physically interesting information, this transformation makes it possible to cut unphysically high eigenvalues and the corresponding eigenvectors from the time propagation scheme, thereby improving its numerical stability and allowing us to use the standard Arnoldi–Lanczos method [8–10] to propagate the initial state in time until the observables of interest can be extracted from the wavefunction.

These observables include the survival probability of the ground state, as well as the probabilities for single-electron excitation and ionization, ionization-excitation, and double ionization. Some of these probabilities are easy to extract via the coefficients of the time-propagated wavefunction in the eigenbasis of the problem, while others require projections to the one-electron or even two-electron continuum. Details can be found in [3–5]. In some cases, it is possible to derive a “generalized cross section” from these probabilities, but care has to be taken in the definition of the “effective interaction time” [11, 12].

3 Example Results

3.1 *Multiphoton Single-Ionization of Neon*

As our first example, Fig. 1 shows the response of the Ne atom to pulses with central photon energies of 11.6 and 7.3 eV, respectively. In these cases, at least two or three photons, respectively, need to be absorbed in order to ionize the system. Since this was our “proof-of-principle attempt” at such a problem, we only used the ground state $(1s^2 2s^2 2p^5)^2P$ of Ne^+ as the target state for the “half collision” of the ejected electron with the residual ion. In order to ensure converged results for the above cases, we actually coupled LS symmetries up to a total orbital angular momentum $L_{\max} = 6$ for the electron–ion collision system. Note that excitation rather than ionization appears as the dominating reaction process for $\omega = 0.27$ a.u. and the laser parameters chosen here.

3.2 *Multiphoton Single-Ionization of Argon*

For the argon target, we performed a more sophisticated calculation [4], in which we coupled three states of the Ar^+ ion. In this project, we studied the effects of the finite pulse length and the intensity on various intermediate resonance states.

Figure 2 depicts the excitation probability at different photon energies. So-called Rabi oscillations occur when the photon energy matches the energy gap between the ground state and, in this case, the $(3p^5 4s)^1P$ excited state. This matching leads

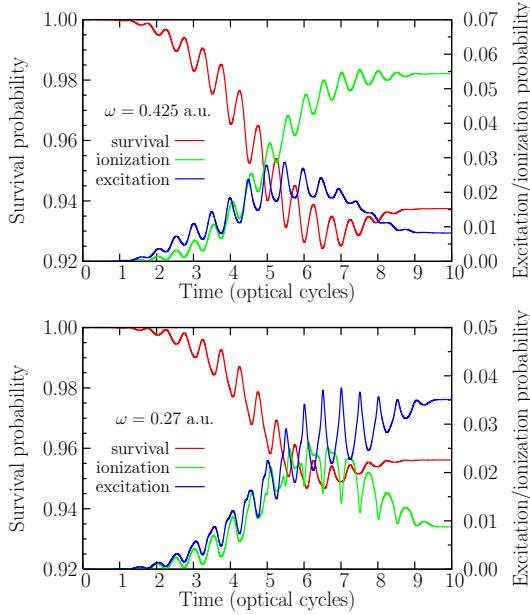
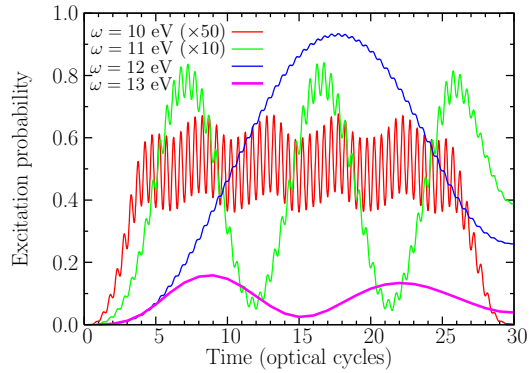


Fig. 1 Ground-state survival (left scale) and total excitation and ionization probabilities (right scale) for Ne exposed to 10-cycle laser pulses of peak intensity $3.5 \times 10^{14} \text{ W/cm}^2$ with a Gaussian envelope. The central laser frequencies are 0.425 a.u. (11.6 eV, top panel) and 0.27 a.u. (7.3 eV, bottom panel).

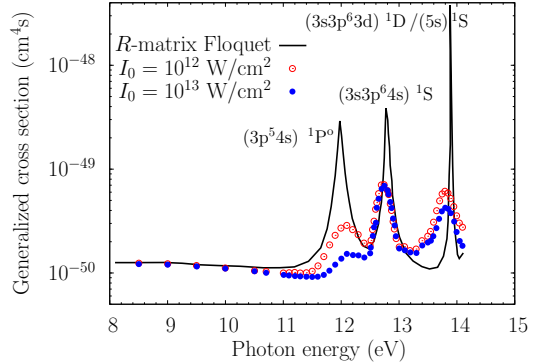
Fig. 2 Excitation probability of argon for a 30-cycle laser pulse with peak intensity of $2 \times 10^{13} \text{ W/cm}^2$ and photon energies of 10, 11, 12, and 13 eV. Note the different scales for the individual photon energies.



to oscillations in the excitation probability with a large amplitude and a long period. There are still oscillations when the photon energy is tuned away from the energy gap, but they have much smaller amplitudes and shorter periods.

As a result of coupling several ionic states, Rydberg-type resonances converging to different thresholds can be observed. However, both the finite length of the pulse and its intensity have an effect on the details of the observed structures. [Figure 3](#) shows the effect of the laser intensity on the generalized two-photon cross sec-

Fig. 3 Effect of the laser peak intensity on the generalized two-photon cross section for a 30-cycle laser pulse interacting with argon. The Floquet-results are from McKenna and van der Hart [13].



tion. While both peak intensities, 10^{12} and 10^{13} W/cm², still lie in the perturbative regime, the height of the first resonance peak is significantly diminished for the more intense laser field. Similar results have been obtained by another time-dependent *R*-matrix approach, which is independently being developed by the Belfast group [14].

Figure 4 exhibits two examples for the single ionization rates in argon [4] obtained in few-cycle laser pulses of different lengths, intensities, and central wavelengths. There is clearly a nontrivial dependence on the various laser parameters, and once again resonances appear when the photon wavelength is varied. These predictions are currently awaiting experimental tests, but they show the richness of effects that can be expected in complex targets where inter-shell correlation effects play an important role.

3.3 Two-Color Two-Photon Double Ionization of Helium

The two-photon double ionization (DI) of the helium atom induced by intense short XUV laser pulses has received considerable attention from both theorists and experimentalists alike. Instead of listing a large number of references here, we note that much of the recent work was quoted in [11, 12], but several additional papers appeared since then or are currently in press. Interestingly, even the calculation of the total cross section for this process is under heavy dispute, with ongoing debates about the need, or lack thereof, to account for the electron-electron interaction in the final state and the role of the direct vs. the sequential process [15]. For more details, we refer to the above references and several papers in the special journal issue headed by [1].

Here we consider the process of double photoionization by absorption of two photons at different central photon energies. In other words, the target helium atom is exposed to the irradiation by two laser pulses, of potentially different frequencies and with a controllable time delay. Specifically, the following two-color laser parameters were used for the results shown in Fig. 5: Pulse 1 has a central photon

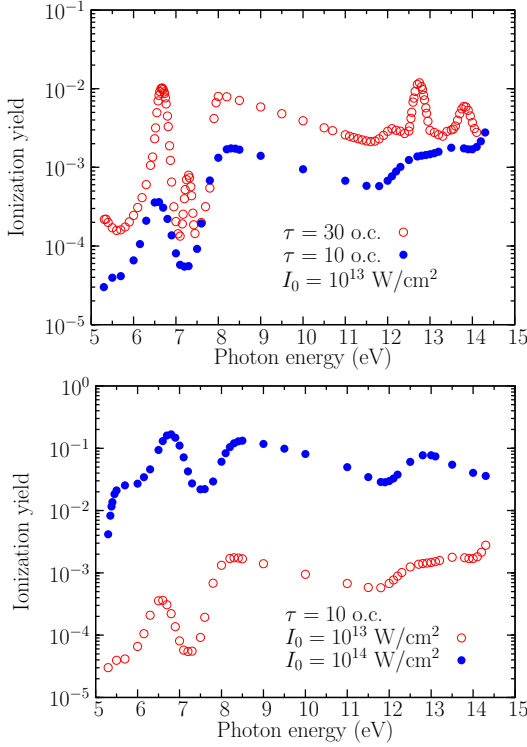


Fig. 4 Ionization yield as a function of photon energy in 10-cycle and 30-cycle laser pulses of peak intensity 10^{13} W/cm^2 (top) and for 10-cycle laser pulses with peak intensities of 10^{13} W/cm^2 and 10^{14} W/cm^2 (bottom).

energy of 35.3 eV and a peak intensity of 10^{14} W/cm^2 , while the corresponding parameters for pulse 2 are 57.1 eV and 10^{13} W/cm^2 , respectively. The length of each pulse is 10 optical cycles with a Gaussian envelope, thus corresponding to pulse lengths of about 1.2 and 0.7 femtoseconds, respectively.

We are interested in the mechanism for the ejection of two electrons when the time delay between the two pulses is varied. We define this delay as the time distance between the peak intensities. Consequently, there is no overlap at all between the two pulses for a delay of about 0.95 femtoseconds, corresponding to a little less than 40 atomic units of time (1 a.u. \approx 24 attoseconds).

Figure 5 shows the results for a variety of delays, ranging from about -120 attoseconds (i.e., the second photon with the higher energy comes first) to 600 attoseconds. Not surprisingly, the probability for double ionization is small in the first case, since the only chance for this process to happen is the two photons working together on the two electrons. Even when the two pulses come simultaneously, the probability for double ejection remains relatively small, and the peak for equal-energy sharing is a clear indication of the direct process. With increasing time delay, the peaks expected for the sequential process – one at 10.7 eV and the other at 2.7 eV, corre-

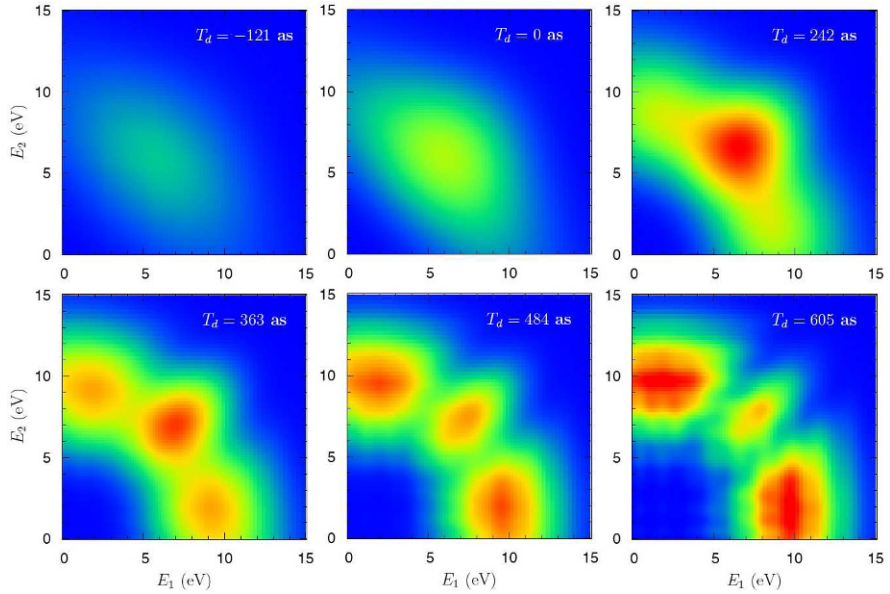


Fig. 5 Energy distributions of the two escaping electrons in two-color laser pulses of 10 optical cycles each. The laser parameters are: $\omega_1 = 35.3$ eV at a peak intensity of 10^{14} W/cm² and $\omega_2 = 57.1$ eV at a peak intensity of 10^{13} W/cm². The delay between the two pulses is varied between -121 as and $+605$ as. See text for details.

sponding to the 35.1 eV photon ionizing the neutral helium atom with an ionization potential of 24.6 eV and the other one ionizing the $\text{He}^+(1s)$ ion with an ionization potential of 54.4 eV – start to grow, but the two processes still have about equal weight for a time delay as large as 400 attoseconds.

From this example, it is clear that the time delay plays a decisive role in determining how the two electrons are ejected by two-color XUV laser pulses. Depending on the details of the time delay, the electrons can be ejected in ways either similar to the sequential or the nonsequential process. Our findings qualitatively agree with those of Fomouuo et al. [16] for the two-color problem and Feist et al. [17] in the single-color problem. They serve as an independent confirmation of their predictions, and also give us confidence in our computer code.

4 Summary and Outlook

We have presented a *general* method to calculate short-pulse intense laser interactions with complex atoms using a *B*-spline *R*-matrix approach in connection with an efficient Arnoldi–Lanczos time propagation scheme. Test calculations for several systems revealed good agreement with previous benchmark results obtained with different and entirely independent methods. Our application to two-photon double

ionization of helium using two time-delayed XUV laser pulses confirmed that attosecond spectroscopy will provide a “microscope” to examine and also control the way electrons interact in atomic and molecular targets.

We are currently in the process of generating and then transforming the corresponding matrices for the two-photon double ionization problem of neon atoms. This will allow us to make a direct comparison with the recent experiments of Moshhammer et al. [18] carried out at the FLASH facility in Hamburg. While the additional complication of a residual core with nonzero angular momentum is substantial, the current method has been formulated in such a way that these calculations are effectively limited by the available hardware (i.e., supercomputer facilities) rather than special-purpose software.

Nevertheless, in order to move to systems like Ne and Ar, we need more work on parallelizing the code and substantial resources to handle the matrices that can quickly reach ranks of 50,000–100,000. To use the eigenbasis, we will need to solve a generalized eigenvalue problem *once* for each partial-wave symmetry, and these matrices are not sparse. However, in light of currently available computational resources, we are confident that we will be able to generate results for complex targets, including simple molecules, in the near future.

Acknowledgements The work presented here was supported by the United States National Science Foundation under grants PHY-0757755 (KB and XG) and PHY-0901838 (KB,OZ,CJN), and supercomputer resources through the Teragrid allocation TG-PHY090031.

References

1. R. Moshhammer, J. Ullrich, J. Phys. B **42**(134001) (2009)
2. M. Uiberacker, T. Uphues, M. Schultze, A.J. Verhoef, V. Yakovlev, M.F. Kling, J. Rauschenberger, N.M. Kabachnik, H. Schröder, M. Lezius, K.L. Kompa, H.G. Muller, M.J.J. Vrakking, S. Hendel, U. Kleineberg, U. Heinzmann, M. Drescher, F. Krausz, Nature **446**, 627 (2007)
3. X. Guan, O. Zatsarinny, K. Bartschat, B.I. Schneider, J. Feist, C.J. Noble, Phys. Rev. A **76**, 053411 (2007)
4. X. Guan, C.J. Noble, O. Zatsarinny, K. Bartschat, B.I. Schneider, Phys. Rev. A **77**, 053402 (2008)
5. X. Guan, O. Zatsarinny, C.J. Noble, K. Bartschat, B.I. Schneider, J. Phys. B **42**, 134015 (2009)
6. O. Zatsarinny, Comput. Phys. Commun. **174**, 273 (2006)
7. X. Guan, C.J. Noble, O. Zatsarinny, K. Bartschat, B.I. Schneider, Comput. Phys. Commun. **180**, 2401 (2009)
8. S. Hutchinson, M.A. Lysaght, H.W. van der Hart, J. Phys. B **42**, 096603 (2010)
9. T.J. Park, J.C. Light, J. Chem. Phys. **85**, 5870 (1986)
10. E.S. Smyth, J.S. Parker, K.T. Taylor, Comput. Phys. Commun. **114**, 1 (1998)
11. X. Guan, K. Bartschat, B.I. Schneider, J. Phys. A **77**, 043421 (2008)
12. J. Feist, S. Nagele, R. Pazourek, E. Persson, B.I. Schneider, L.A. Collins, J. Burgdörfer, Phys. Rev. A **77**, 043420 (2008)
13. C. McKenna, H.W. van der Hart, J. Phys. B **37**, 457 (2004)
14. M.A. Lysaght, H.W. van der Hart, P.G. Burke, Phys. Rev. Lett. **101**, 25301 (2008)
15. P. Lambropoulos, L.A.A. Nikopoulos, M.G. Makris, A. Mihelic, Phys. Rev. A **78**, 055402 (2008)

16. E. Fomouuo, P. Antoine, H. Bachau, B. Pireaux, *New J. Phys.* **10**, 025017 (2008)
17. J. Feist, S. Nagele, R. Pazourek, E. Persson, B.I. Schneider, L.A. Collins, J. Burgdörfer, *Phys. Rev. Lett.* **103**, 063002 (2009)
18. R. Moshhammer, Y.H. Jiang, L. Foucar, A. Rudenko, T. Ergler, C.D. Schröter, S. Lüdemann, K. Zrost, D. Fischer, J. Titze, T. Jahnke, M. Schöffler, T. Weber, R. Dörner, T.J.M. Zouros, A. Dorn, T. Ferger, K.U. Kühnel, S. Düsterer, R. Treusch, P. Radcliffe, E. Plönjes, J. Ullrich, *Phys. Rev. Lett.* **98**, 203001 (2007)

Quantum Dynamic Imaging
Theoretical and Numerical Methods
Bandrauk, A.D.; Ivanov, M. (Eds.)
2011, XVI, 236 p., Hardcover
ISBN: 978-1-4419-9490-5